

The Phase Diagram of the Quasiternary System (Sn, Pb) (S, Te)

Volkmar Leute, S. Brinkmann, J. Linnenbrink and H. M. Schmidtke

Institut für Physikalische Chemie der Universität Münster, Schlossplatz 4, D-48149 Münster

Z. Naturforsch. **50a**, 459–467 (1995); received November 30, 1994

Dedicated to Prof. Dr. E. Wicke on occasion of his 80th birthday

The phase diagram of the quasiternary system $(\text{Sn}_k \text{Pb}_{1-k})(\text{S}_l \text{Te}_{1-l})$ for 900 K is determined by X-ray diffraction and by electron microprobe analysis. Moreover, the free enthalpy faces $g(k, l)$ for the phases with cubic rocksalt structure (cub) or with the orthorhombic SnS structure (orh) are calculated from the interaction parameters and from the orh \rightarrow cub transition data of the 4 quasibinary subsystems.

The interaction parameters are also used to calculate the thermodynamic factor for interdiffusion along quasibinary sections through the phase square and to calculate the energies of four-particle clusters. By application of the cluster model one obtains information on the local environment of the mixing particles and on the cluster processes that have effect upon interdiffusion.

1. Introduction

There are many investigations on optical properties of quasibinary or quasiternary solid solutions of IV–VI semiconductors in connection with their application for the development of tunable diode lasers [1]. But on the phase diagrams of these systems only a few papers were published. Even for the quasibinary systems the thermodynamic properties are often merely fragmentarily known.

Only if the extensions of the spinodal and structural miscibility gaps are known, the range of possible stable compositions and the most suitable preparation conditions for alloys with desired properties can carefully be chosen.

For those systems, for which the thermodynamic mixing properties of the quasibinary subsystems of a quasiternary system of type $(\text{M}, \text{N})(\text{X}, \text{Y})$ are known, it is possible to determine the phase diagram of the quasiternary system by calculation [2]. We will show in this paper that for the rather complicated system $(\text{Sn}_k \text{Pb}_{1-k})(\text{S}_l \text{Te}_{1-l})$ the experimentally determined and the calculated phase diagrams are in good accordance.

As to the quasibinary subsystems, each of the four phase diagrams shows a different topology. The most ideal system $(\text{Sn}, \text{Pb})\text{Te}$ yields complete solid solubility even at rather low temperatures [3]. The system $\text{Pb}(\text{S}, \text{Te})$ shows a spinodal miscibility gap at temperatures lower than 1073 K [4]. It is known that SnS crys-

tallizes in an orthorhombic lattice, whereas the other three binary compounds show the cubic rocksalt structure. Thus, the two systems that include the component SnS must show a structural miscibility gap. In $\text{Sn}(\text{S}, \text{Te})$ this miscibility gap is very broad, yielding an eutectic behaviour, whereas in the system $(\text{Sn}, \text{Pb})\text{S}$, in the temperature region $850 \text{ K} < T < 1150 \text{ K}$, a narrow structural miscibility gap between the cubic and orthorhombic phases occurs together with a spinodal miscibility gap within the orthorhombic phase [5].

The energies of four-particle clusters can be calculated, provided the interaction parameters of the quasibinary systems are given as linear functions of the mole fractions k or l [6]. From these cluster energies we can calculate the cluster probabilities, which give information about the probability of finding a special local composition around a given particle. Within the scope of the cluster model the elementary diffusion processes can be regarded as exchange reactions between adjacent clusters.

2. Experimental Determination of the Phase Diagram

2.1. Initial Substances

The binary compounds PbS, PbTe, SnS and SnTe were synthesized from the elements (purity: 99.999%) in evacuated quartz ampoules. The lead chalcogenides were purified by sublimation in dynamic vacuum: PbTe at 1073 K, PbS twice at 1223 K. The tin chalcogenides, which do not sublime congruently, were purified by vertical zone refining: SnS between

Reprint requests to Prof. V. Leute.

0932-0784 / 95 / 0400-0459 \$ 06.00 © – Verlag der Zeitschrift für Naturforschung, D-72027 Tübingen



Dieses Werk wurde im Jahr 2013 vom Verlag Zeitschrift für Naturforschung in Zusammenarbeit mit der Max-Planck-Gesellschaft zur Förderung der Wissenschaften e.V. digitalisiert und unter folgender Lizenz veröffentlicht: Creative Commons Namensnennung-Keine Bearbeitung 3.0 Deutschland Lizenz.

Zum 01.01.2015 ist eine Anpassung der Lizenzbedingungen (Entfall der Creative Commons Lizenzbedingung „Keine Bearbeitung“) beabsichtigt, um eine Nachnutzung auch im Rahmen zukünftiger wissenschaftlicher Nutzungsformen zu ermöglichen.

This work has been digitalized and published in 2013 by Verlag Zeitschrift für Naturforschung in cooperation with the Max Planck Society for the Advancement of Science under a Creative Commons Attribution-NoDerivs 3.0 Germany License.

On 01.01.2015 it is planned to change the License Conditions (the removal of the Creative Commons License condition “no derivative works”). This is to allow reuse in the area of future scientific usage.

1223 K and 1123 K, SnTe between 1123 K and 1013 K, both with a pulling rate of 2.2 cm/day.

2.2. X-ray Measurements and Electron Microprobe Analysis

To determine for the different regions of solid solutions the lattice constant in dependence on composition we prepared several sets of powder mixtures of different mole ratios of the pure binary components. All samples, sealed in evacuated quartz ampoules, were homogenized for 24 hours at 1350 K. Subsequently, the samples were annealed at 900 K for about 3 weeks. Then the ampoules were quenched to room temperature by dipping in ice water.

Afterwards one part of the samples was investigated by the X-ray Guinier method. Besides the homogeneous samples that showed a single pattern of cubic or orthorhombic reflections there were two-phase samples showing both patterns simultaneously. Some samples that suffered a spinodal demixing during equilibration showed twofold sets of cubic or of orthorhombic reflections. Moreover, in some composition regions we found three-phase samples showing one orthorhombic and two cubic or one cubic and two orthorhombic sets of reflections.

The homogeneous samples, with a single sharp reflection pattern, were used to find quantitative descriptions for the composition dependence of the lattice constants. For the telluride rich quasiternary solid solution with cubic structure the lattice constant $a(k, l)$ can be described by a polynomial with 4 coefficients:

$$a(k, l)/\text{pm} = 646.16 - 14.26k - 46.87l + 14.92kl \quad (1)$$

For the sulfide rich region of the phase diagram with orthorhombic structure the lattice constants can be given by three coefficients:

$$a(k, l)/\text{pm} = 470.77 + 12.18k - 50.0l \quad (2)$$

$$b(k, l)/\text{pm} = 1265.57 - 47.06k - 99.0l \quad (3)$$

$$c(k, l)/\text{pm} = 471.60 - 21.55k - 52.0l \quad (4)$$

The polynomials (1)–(4) will be used to obtain information on the equilibrium compositions of those samples that separated by equilibration into two or three solid solutions of different composition.

Additional information was obtained from measurements of two- or three-phase samples by an elec-

tron microprobe. Often, the particle sizes of the crystallites in heterogeneous samples are too small to obtain the exact composition of the equilibrium phases by measurements with the electron microprobe at selected positions on the sample surface. But even if the cross section of the electron beam covers crystallites of both phases, the measured mean composition has to be situated on the tie line between two points of equilibrium composition in the phase diagram. Thus, from many measurements with the electron microprobe on a heterogeneous sample one can determine a cloud of composition points within the two-phase region. If these points are fitted to a straight line, the slope of this line can be identified with the slope of the equilibrium tie line, and the utmost ends of the cloud in direction of the tie line give a good approximation of the equilibrium compositions. In three-phase samples the measured data points culminate near the corners and the edges of the corresponding three-phase triangle (cf. Figure 1).

If the direction of a tie line is known, the equilibrium endpoints of this tie line can be determined from the measured lattice constants by use of (1)–(4). With the same methods, the composition corresponding to the corners of the three-phase regions can be determined from the tie line fields and from the lattice constants derived from the three-phase samples.

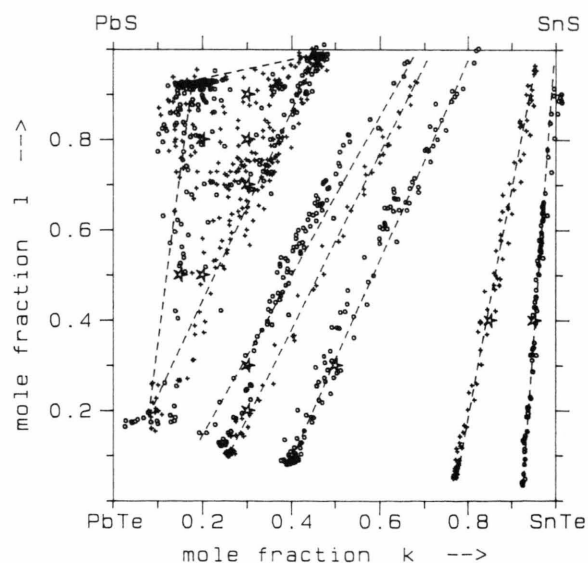


Fig. 1. Data points measured with the electron microprobe on samples that separated into a sulfide rich orthorhombic phase and a telluride rich cubic phase or into three phases after annealing at $T=900$ K. * overall composition of the samples.

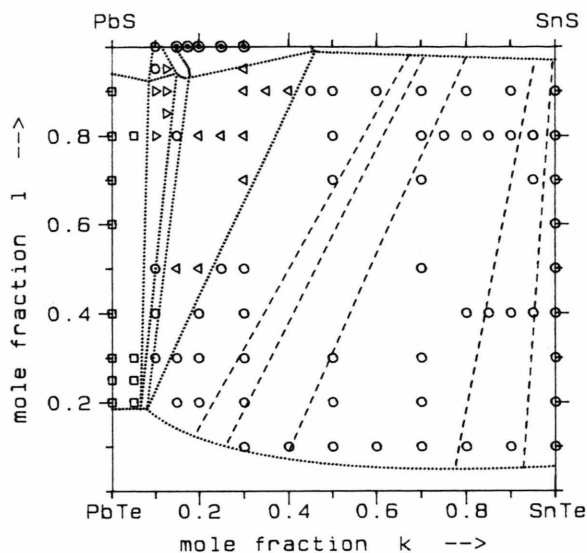


Fig. 2. The phase diagram of the quasiternary system $(\text{Sn}_k \text{Pb}_{1-k})(\text{S}_i \text{Te}_{1-i})$ as experimentally determined by X-ray diffraction and by electron microprobe analysis on samples annealed at $T=900$ K. All data points corresponding to the overall compositions of samples that have separated after equilibration into multi-phase samples with \square two 'cub' phases, \circ one 'orh' and one 'cub' phase, \diamond two 'orh' phases, \triangle two 'orh' and one 'cub' phase, ∇ one 'orh' and two 'cub' phases.

Figure 2 shows the phase diagram of the quasiternary system $(\text{Sn}_k \text{Pb}_{1-k})(\text{S}_i \text{Te}_{1-i})$ as derived from X-ray measurements, electron microprobe analysis and from the analysis of backscatter electron images.

3. Calculation of the Phase Diagram

3.1. Transition Data and Reaction Parameters

As shown in previous papers [2, 7] the mean molar excess free enthalpy $g^E(k, l)$ for a phase of a quasiternary system can be derived from the interaction parameters of the quasibinary edge systems. The only ternary parameter needed for these calculations is the standard free enthalpy $\Delta_R G^0$ of the solid state reaction between the pure binary components. For the given quasiternary system this reaction is described by:



For this reaction between the components being in their stable phases $\Delta_R G^0$ can be calculated from the standard formation enthalpies and entropies of the

pure binary components as given by Abrikosov [8]. If the excess free enthalpy face $g^E(k, l)^\Phi$ is to be calculated for a given phase Φ , then however, all four binary components must belong to this phase Φ . Thus, we have to transform the formation values as well as the interaction parameters to phase Φ . For that reason we need for the binary components the enthalpies and entropies of transition from the orthorhombic to the cubic phase. These transition data are listed in Table 1.

All transition data, except those for PbTe, were already determined in previous papers. From the phase sequence for increasing temperature: zbl (zinc-blende) \rightarrow orh \rightarrow cub [9], it follows that the temperature for the zbl \rightarrow cub transition of PbTe ($T_T \approx 310$ K), which was estimated in [10], may not be higher than that for its orh \rightarrow cub transition. Moreover, the transition entropies for PbTe and SnTe should be nearly equal, because both compounds form nearly ideal solid solutions even at low temperatures. On this basis we obtained for the transition data of PbTe the values given in Table 1.

Using these transition data the standard values $\Delta_R H^0$ and $\Delta_R S^0$ for the reaction given by (5) can be converted into values for the reactions in which the components are all in the cubic or all in the orthorhombic phase (Table 2). The procedure for these calculations has been described in [7].

3.2. Interaction Parameters

The interaction parameters for the cubic quasibinary subsystem Pb(S, Te) [4] and for the subsystem

Table 1. Transition data.

Substance	SnS	PbS	PbTe	SnTe
$\Delta_{Tr} H_0 \left/ \left(\frac{\text{kJ}}{\text{mol}} \right) \right.$	6.0 [5]	0.02 [5]	0.22	0.21 [9]
$\Delta_{Tr} S_0 \left/ \left(\frac{\text{J}}{\text{K} \cdot \text{mol}} \right) \right.$	0.70 [5]	0.14 [5]	0.70	0.70 [9]

Table 2. Standard reaction parameters.

Phase	Eq. (5)	Orthorhombic	Cubic
$\Delta_R H_0 \left/ \left(\frac{\text{kJ}}{\text{mol}} \right) \right.$	20.95	20.94	14.95
$\Delta_R S_0 \left/ \left(\frac{\text{J}}{\text{K} \cdot \text{mol}} \right) \right.$	5.44	5.30	4.74

(Sn,Pb)S in the cubic as well as in the orthorhombic phase [5] are already published.

For the system $(\text{Sn}_k\text{Pb}_{1-k})\text{Te}$, we determined the solidus curve by DTA measurements. From these data we could show that the mixing behaviour of this system is even more ideal than reported by Laugier [3]. The deviation from ideal behaviour increases very slightly with increasing SnTe content. For the calculation of the interaction parameter in the cubic phase (cf. Table 3) we used also the fusion data as listed in Table 4.

In [7] we have shown that if the transformation data (Table 1) are known, the interaction parameters can be converted into values for an other phase. This possibility we have used to estimate for the orthorhombic phases of (Sn,Pb)Te and of Pb(S,Te) the interaction parameters (Table 3) that could not be obtained directly from quasibinary phase diagrams.

As to the system $\text{Sn}(\text{S}_l\text{Te}_{1-l})$, we know from our measurements with the electron microprobe that near the eutectic temperature a broad miscibility gap extends from $l=0.06$ up to $l=0.96$. According to measurements by Nasirov [16], the composition of the melt at the eutectic temperature ($T_E=960$ K) corresponds to $l_E^{\text{liq}}=0.53$. By adjustment of the interaction parameters for the cubic and orthorhombic phases we calculated a phase diagram that corresponds with the eutectic data and with the melting points of the pure binary components. For this calculation we used the fusion data of Table 4 and the transition data given in Table 1. The resulting interaction parameters are listed in Table 3.

Table 3. Interaction parameters.

System	$\alpha / \frac{\text{kJ}}{\text{mol}}$	$\beta / \frac{\text{kJ}}{\text{mol}}$
$(\text{Sn}, \text{Pb})\text{Te}^{\text{cub}}$	0	0.25
$(\text{Sn}, \text{Pb})\text{Te}^{\text{orh}}$	0	0.26
$\text{Sn}(\text{S}, \text{Te})^{\text{cub}}$	-91.0	911.6
$\text{Sn}(\text{S}, \text{Te})^{\text{orh}}$	338.7	-342.8
$\text{Sn}(\text{S}, \text{Te})^{\text{liq}}$	-5.0	0
$\text{Pb}(\text{S}, \text{Te})^{\text{orh}}$	25.5	10.7

Table 4. Thermodynamic data of fusion.

Substance	SnTe	PbTe	SnS
$\Delta_F H_0 / \left(\frac{\text{kJ}}{\text{mol}} \right)$	34.0 [11]	39.3 [12]	31.6 [8]
T_F / K	1078 [13]	1198 [14]	1153 [15]

3.3. Calculation of Tie Line Fields

The data listed in Tables 1–3 are derived exclusively from properties of the quasibinary subsystems or of the pure binary components. To check if the behaviour of the quasiternary system $(\text{Sn}_k\text{Pb}_{1-k})(\text{S}_l\text{Te}_{1-l})$ can be described by these data, we have to calculate the phase diagram and to compare it with the experimentally determined phase diagram.

The essential characteristics of a quasiternary phase diagram are the equilibrium tie line fields for the structural and spinodal miscibility gaps. To calculate these fields, the mean molar free enthalpy functions $g^\Phi(k, l)$ for both phases $\Phi \in \{\text{orh}, \text{cub}\}$ have to be determined. The equations for these calculations are described in detail in [2]. With the indices I and II characterizing the equilibrium compositions at the endpoints of a tie line, the equilibrium conditions are given by

$$\left(\frac{\partial g}{\partial k} \right)^I = \left(\frac{\partial g}{\partial k} \right)^{II}, \quad (6)$$

$$\left(\frac{\partial g}{\partial l} \right)^I = \left(\frac{\partial g}{\partial l} \right)^{II}, \quad (7)$$

$$g^I - k^I \left(\frac{\partial g}{\partial k} \right)^I - l^I \left(\frac{\partial g}{\partial l} \right)^I = g^{II} - k^{II} \left(\frac{\partial g}{\partial k} \right)^{II} - l^{II} \left(\frac{\partial g}{\partial l} \right)^{II}. \quad (8)$$

If a tie line field describes a spinodal miscibility gap, then both endpoints of the tie line belong to the same phase, cubic (cub) or orthorhombic (orh). In the case of a structural miscibility gap (cub/orh), however, one endpoint of a tie line belongs to the cubic the other to the orthorhombic phase.

We have calculated two (cub/orh) fields and one (orh/orh) field forming the boundaries of a (cub/orh/orh) three-phase triangle (cf. Figure 3a). Furthermore, we calculated two different (cub/cub) fields and a third, very narrow (cub/orh) field. These additional two-phase fields give rise to two (cub/cub/orh) three-phase triangles: one triangle very narrow in k direction, but extending over a broad l -range, and one tiny triangle near the PbS corner (cf. Figure 3b).

4. Comparison of Experimentally Determined and Calculated Phase Diagrams

Figures 3a and b show plots of the calculated phase diagram for $T=900$ K. The positions of the point

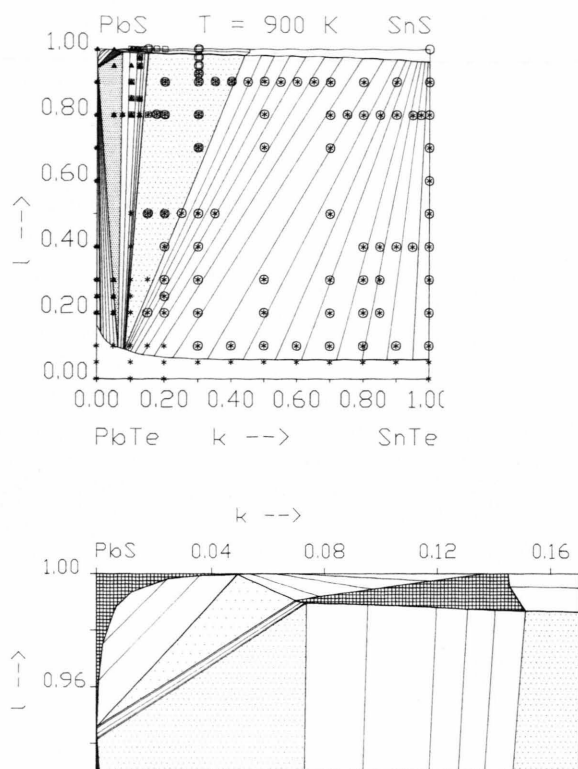


Fig. 3. The phase diagram of the quasiternary system $(\text{Sn}_k \text{Pb}_{1-k})(\text{S}_l \text{Te}_{1-l})$ as calculated from the thermodynamic data of the quasibinary subsystems. Full straight lines = tie lines between equilibrium points, dotted regions = three-phase triangles constructed from overlapping tie line fields. Part (a) shows the whole isothermal section for $T = 900 \text{ K}$, part (b) the calculated details near the PbS rich corner. The point symbols in (a) correspond to X-ray patterns that show a line set of the * telluride rich cubic phase, Δ PbS rich cubic phase, \circ SnS rich orthorhombic phase, \square PbS rich orthorhombic phase. Multiphase samples are indicated by two or three of these symbols.

symbols, included in Fig. 3a, correspond to the overall composition of the samples used for the X-ray measurements. With exception of the region $0 < k < 0.1$ the calculated diagram correlates very well with the X-ray results. A comparison with Fig. 2 reveals also a good accordance of the topology of the calculated with that of the experimentally determined phase diagram. The only discrepancies between calculated and experimentally determined phase diagrams appear in the region $0.1 \leq k \leq 0.125$, $0.8 \leq l \leq 0.95$. X-ray patterns of samples with an overall composition within this region show some reflections that can be interpreted as belonging to the PbS rich cubic phase. But, according to the cal-

culated tie line fields this region should belong to the (cub/orh) two-phase region between the (cub/orh/orh) and (cub/cub/orh) triangles. If the rather difficult interpretation of the X-ray patterns of these samples should be correct, the right side of the (cub/cub/orh) triangle has to drift a distance of $\Delta k \approx 0.05$ to higher k values than found by calculation. This drift would occur at the expense of the adjacent (cub/orh) two-phase region that should become narrower.

Figure 3b is a part of the calculated phase diagram shown in Fig. 3a and describes the surroundings of the tiny (cub/cub/orh) triangle that could not be detected experimentally. But its existence is suggested by the topology of the phase diagram.

5. Clusters

Generally, solid solutions are described as mixtures of monoatomic particles, for example, the quasibinary solution $\text{Sn}(\text{S}, \text{Te})$ as a mixture of S and Te particles within an Sn matrix. The mixing entropy is simply taken as the configuration entropy and the deviation from ideal mixing behaviour is totally described by the so-called interaction parameter. This description does not consider the local neighbourhood of a given particle. If, however, the mixture is described as an ideal solution of clusters, the environment of a particle can be considered the better, the more particles a cluster encloses. But, with increasing cluster size, the number of different clusters, and thus, the difficulties in solving the calculation problems increase rather rapidly.

The four-particle clusters in our model are three-sided pyramids with three particles of one sublattice at the base plane and one particle of the other sublattice at the apex of the pyramid, as for example SnSSS , SnSSTe , SnSTeTe and SnTeTeTe [6]. The octahedral seven-particle clusters that would consider all nearest neighbours in the rocksalt lattice can be split into 8 of these pyramidal clusters. The consideration of pyramidal clusters corresponds with a description by interaction parameters that depend linearly on composition. That means that good approximations for the energies of pyramidal clusters can be derived from such interaction parameters, provided the random distribution assumption is not violated too much.

If the cluster energies are known, the standard enthalpies for reactions between clusters and the probability distributions for the clusters can be calculated. The quasibinary systems $\text{Pb}(\text{S}, \text{Te})$ and $(\text{Sn}, \text{Pb})\text{S}$ were

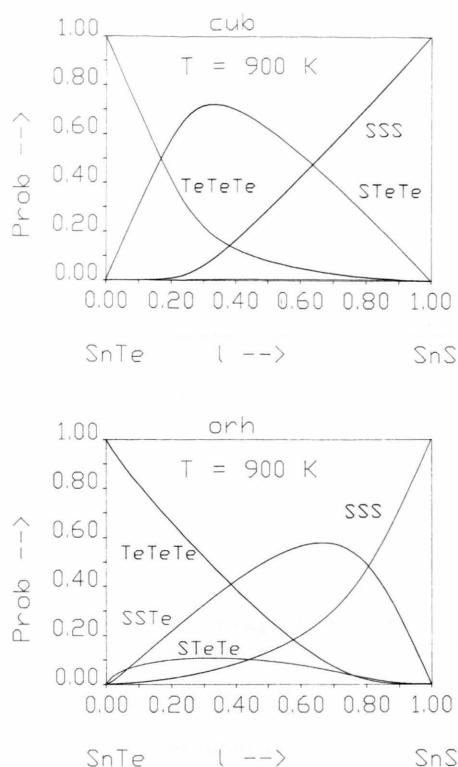


Fig. 4. Absolute probabilities at $T=900$ K for the 4 pyramidal clusters of the quasibinary system $\text{Sn}(\text{S}_i\text{Te}_{1-i})$ in dependence on the sulfide mole fractions l . (a) for the cubic, (b) for the orthorhombic phase.

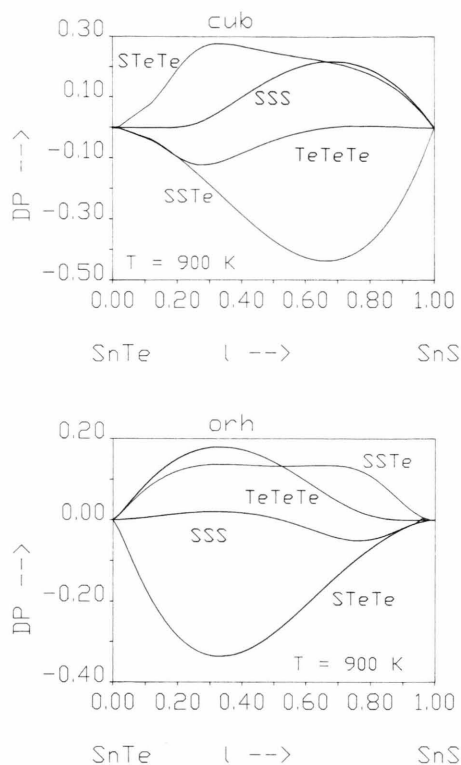


Fig. 5. Differences DP between the energy dependent cluster probabilities of Fig. 4 and cluster probabilities calculated on the random distribution assumption. (a) for the cubic, (b) for the orthorhombic phase.

already discussed on the basis of this cluster model in [6] and [5]. For these systems, it was shown that the maximum deviation of cluster probabilities from random cluster distribution does not exceed 0.025.

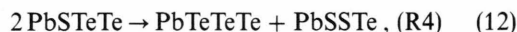
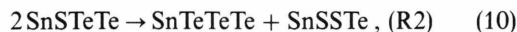
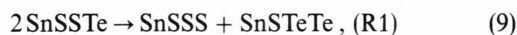
For the nearly ideal system $(\text{Sn}, \text{Pb})\text{Te}$ any deviation from random cluster distribution can be neglected.

In the eutectic system $\text{Sn}(\text{S}, \text{Te})$, however, the interaction parameters are so high that considerable deviations are to be expected. In Fig. 4a, b the absolute cluster probabilities for the cubic (cub) and the orthorhombic (orh) quasibinary system $\text{Sn}(\text{S}_i\text{Te}_{1-i})$ are plotted as function of the sulfide mole fraction l . Figs. 5a, b show the corresponding differences between these absolute probabilities and the probabilities in the case of random distribution within an ideal solid solution.

The energies of the 4-particle clusters, as calculated from the free formation enthalpies, the free transition enthalpies, and the interaction parameters for the

cubic and orthorhombic phases, are listed in Table 5 in the form of averaged cluster energies as defined in [6].

The free standard enthalpies for the cluster reactions within the chalcogen sublattice



as calculated from the averaged cluster energies in Table 5, are listed in Table 6.

The very high positive value for the energy of the SnSTeTe cluster in the solid solution with orthorhombic structure (cf. Table 5) causes a high positive $\Delta_{\text{R1}} G^0$ value for the formation of TeTe-pairs within an orthorhombic sulfide rich matrix (cf. Table 6). As expected, the probability for the SnSTeTe cluster in real

Table 5. Cluster energies.

Cluster MXYZ	SnSSS	SnSSTe	SnSTeTe	SnTeTeTe
$\langle E^{\text{orh}} \rangle / \left(\frac{\text{kJ}}{\text{mol}} \right)$	-12.42	-10.91	5.06	-7.37
$\langle E^{\text{cub}} \rangle / \left(\frac{\text{kJ}}{\text{mol}} \right)$	-11.75	23.89	-12.66	-7.43
Cluster NXYZ	PbSSS	PbSSTe	PbSTeTe	PbTeTeTe
$\langle E^{\text{orh}} \rangle / \left(\frac{\text{kJ}}{\text{mol}} \right)$	-11.14	-8.62	-8.06	-8.11
$\langle E^{\text{cub}} \rangle / \left(\frac{\text{kJ}}{\text{mol}} \right)$	-11.15	-9.19	-8.50	-8.16
Cluster MNPX	SnSnSnS	SnSnPbS	SnPbPbS	PbPbPbS
$\langle E^{\text{orh}} \rangle / \left(\frac{\text{kJ}}{\text{mol}} \right)$	-12.42	-11.82	-10.82	-11.14
$\langle E^{\text{cub}} \rangle / \left(\frac{\text{kJ}}{\text{mol}} \right)$	-11.75	-11.37	-10.83	-11.15
Cluster MNPY	SnSnSnTe	SnSnPbTe	SnPbPbTe	PbPbPbTe
$\langle E^{\text{orh}} \rangle / \left(\frac{\text{kJ}}{\text{mol}} \right)$	-7.37	-7.61	-7.87	-8.11
$\langle E^{\text{cub}} \rangle / \left(\frac{\text{kJ}}{\text{mol}} \right)$	-7.43	-7.66	-7.92	-8.16

SnS rich mixtures is much lower than for ideal mixtures with the same composition (cf. Figure 5a). Within the existence region of the orthorhombic phase at 900 K, SnSTeTe or SnTeTeTe clusters do practically not occur (cf. Figure 4a).

As to the cubic phase of the $\text{Sn}(\text{S}_l\text{Te}_{1-l})$ system the situation is equivalent. Here, the energy for the cluster SnSSTe is by far the most positive (cf. Table 5), and the probability for the formation of SS-pairs in a telluride rich matrix (R2) is negligible (cf. Table 6). Thus, in the whole existence region of SnTe rich mixtures, the probability of SnSTeTe clusters is extremely lowered compared to the average distribution probability (cf. Figure 5b). SnTe rich solid solutions are composed exclusively of SnTeTeTe and SnSTeTe clusters. Figure 5a shows that, even if mixtures with much higher sulfide content could be realized, nevertheless, the content of SnSSTe clusters would be negligible.

6. The Thermodynamic Factor

The influence of the thermodynamic properties of a quasibinary solid solution on the interdiffusion coefficient of the particles in the mixed sublattice is generally described by the so-called thermodynamic factor F :

$$\tilde{D} = (x_1 D_2 + x_2 D_1) F. \quad (13)$$

If the excess free enthalpy function $g^E(x_2)$ is known, the activity coefficient can be calculated according to:

$$RT \ln \gamma_1 = g^E - x_2 \left(\frac{\partial g^E}{\partial x_2} \right) \quad (14)$$

Thus, as the thermodynamic factor depends on the first derivative of the activity coefficient:

$$F = 1 - (1 - x_2) \left(\frac{\partial \ln \gamma_1}{\partial x_2} \right), \quad (15)$$

it will be a linear function of the curvature of the free excess enthalpy:

$$F = 1 + \frac{x_2(1 - x_2)}{RT} \left(\frac{\partial^2 g^E}{\partial x_2^2} \right). \quad (16)$$

With $x_2 = k$ or $x_2 = l$, one obtains the thermodynamic factor for the quasibinary subsystems. For the interdiffusion process the thermodynamic factor F considers the additional driving force that is caused by the nonvanishing gradient of the activity coefficient in nonideal solid solutions. As long as the cross effects in ternary systems can be neglected, these relations can also be used for other quasibinary sections with fixed k or l , i.e. for sections parallel to one of the edges of the quasiternary system. In these cases the partial derivatives at constant k or l have to be used in (16).

On the quasibinary section (Sn, Pb)Te the deviation of the thermodynamic factor from the ideal value, $F = 1$, is practically negligible, and also for quasiternary sections with low constant sulfide content the thermodynamic influence on the interdiffusion can be neglected (cf. Figure 6a). Thus, the interdiffusion of Sn and Pb within the whole solubility region of the telluride rich solid solutions can be treated as behaving ideally.

Phase	$\Delta_{R1} G^0 / \left(\frac{\text{kJ}}{\text{mol}} \right)$	$\Delta_{R2} G^0 / \left(\frac{\text{kJ}}{\text{mol}} \right)$	$\Delta_{R3} G^0 / \left(\frac{\text{kJ}}{\text{mol}} \right)$	$\Delta_{R4} G^0 / \left(\frac{\text{kJ}}{\text{mol}} \right)$
cub	-72.2	41.8	-1.28	-0.35
orh	14.4	-28.4	-1.95	-0.62

Table 6. Free standard reaction enthalpies.

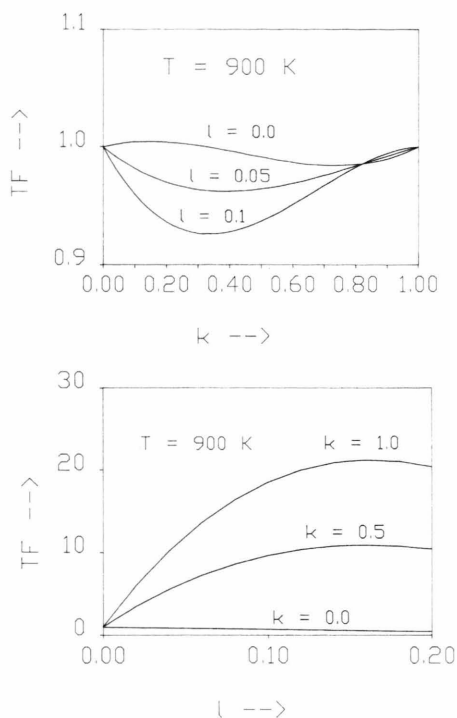


Fig. 6. Thermodynamic factor TF (a) in dependence on the mole fraction k for three quasibinary sections at constant mole fractions l , (b) in dependence on the mole fraction l for three quasibinary sections at constant mole fractions k . The curves are calculated by use of (16).

If, however, the thermodynamic factor is calculated for sections perpendicular to the (Sn, Pb)Te edge, then considerable deviations from ideal behaviour are indicated. For $k=0$, on the Pb(S, Te) edge of the phase square, F decreases with increasing sulfide content because of the spinodal miscibility gap extending between $l \approx 0.18$ and $l \approx 0.94$.

For sections at $k > 0$, the thermodynamic factor increases very rapidly with increasing k , yielding values of $F \geq 1$ already at small Sn chalcogenide contents. Although the solubility for sulfides in the cubic Pb(S, Te) alloys is restricted to values of $l < 0.1$, the thermodynamic factor for the chalcogen interdiffusion in Sn chalcogenide rich solutions increases with increasing sulfide content up to values of $F \approx 10$ near the border of the solubility region. Thus, the exchange of tellurium against sulfur will occur in these alloys more than 10 times faster than expected from the tracer diffusion coefficients.

This surprising behaviour can be understood on the basis of the cluster model. As shown in [5], the thermodynamic factor in quasibinary systems can be described also in terms of the free standard enthalpies of two cluster reactions as (R1), (9) and (R2), (10) or (R3), (11) and (R4), (12), respectively:

$$F(x_2, T) = 1 + \frac{6x_2(1-x_2)}{RT} f(x_2 \Delta_{RA} G^0 + (1-x_2) \Delta_{RB} G^0). \quad (17)$$

Here, $x_2 \in \{l, k\}$ and $f=8$ for octahedrally coordinated lattices.

For quasibinary sections at constant k , the composition variable x_2 in (17) has to be substituted by the mole fraction l . For the Sn and Pb chalcogenides, the corresponding $\Delta_{Ri} G^0$ values are listed in Table 6.

At small l values, the value for the thermodynamic factor is dominated by the second term in the energy sum of (17), i.e. in the case of $k=1$ by the formation energy for the very unstable SS pairs (R2). The high positive $\Delta_{R2} G^0$ value will cause a steep increase of the thermodynamic factor at low sulfide contents (cf. Figure 6b). Thus, the predicted enhancement of the coefficient for the interdiffusion of S and Te in the Sn chalcogenide alloys is connected with the instability of the SS pairs. The additional thermodynamic driving force is the higher, the more the equilibrium of the SS pair formation is shifted to the left side of (10), i.e. to isolated S particles.

For Pb chalcogenides ($k=0$), both energy terms in (17) are negative. In such mixtures, the thermodynamic factor will always be smaller than 1. For this system, $\Delta_{R4} G^0$ determines the behaviour of the thermodynamic factor at small sulfide mole fractions l , and the negative value of $\Delta_{R4} G^0$ shows that in this case the formation of SS pairs is energetically favoured. Thus, the chalcogen interdiffusion is hindered, because the sulfur atoms tend to associate to pairs. With increasing sulfide content this tendency effects that the interdiffusion coefficient decreases more and more until at the spinodal miscibility gap the interdiffusion disappears, i.e. $\bar{D}=0$.

Thus, with increasing Sn chalcogenide content, the effect of the thermodynamic factor changes from hindering the chalcogen interdiffusion in Pb chalcogenide rich alloys to favouring this interdiffusion in Sn chalcogenide rich alloys (cf. Figure 6b).

7. Conclusions

The thermodynamic behaviour of the quasiternary system is characterized on the one side by the fact that in all quasibinary systems, except the system Sn(S, Te), the interaction parameters have nearly the same values for both cubic and orthorhombic phases, and on the other side by the fact that the interaction within the chalcogen sublattice is distinctly higher than within the metal sublattice. This latter effect may be caused by the greater relative difference in the radii for S and Te than for Sn and Pb (covalent radii/pm: $r_S = 104$, $r_{Te} = 137$, $r_{Sn} = 140$, $r_{Pb} = 154$ [17]. These ratios are reflected by the ratios of the cubic lattice constants ($a_{PbTe}/a_{PbS} = 1.088$, $a_{PbTe}/a_{SnTe} = 1.023$).

These geometrical relations are also the reason why, within the quasiternary alloys, the interaction increases with increasing sulfide content. That means that in solutions with a high sulfide content the substi-

tution of S by Te, and to a smaller degree also of Sn by Pb, will cause higher local lattice strains than in solutions with a high telluride content.

Most probably, the behaviour of the chalcogen interactions is responsible for the broad miscibility gaps between sulfide rich and telluride rich alloys and for the fact that the spinodal miscibility gaps pass into three-phase triangles extending over great distances in the mole fraction l .

The positive slope of the tie lines between the cubic and the orthorhombic phases follows consequently from the positive value (cf. Table 2) for the free standard enthalpy $\Delta_R H_0$ of the reaction given in (5).

Acknowledgements

Financial support of this work by the Deutsche Forschungsgemeinschaft and by the Fonds der Chemischen Industrie is acknowledged.

- [1] "Monitoring of Gaseous Pollutants by Tunable Diode Lasers", Editors: R. Grisar, H. Böttner, M. Tacke and G. Restelli, Kluwer Acad. Publishers, Dordrecht 1992.
- [2] V. Leute, Ber. Bunsenges. Phys. Chem. **93**, 7 (1989).
- [3] A. Laugier, Rev. Phys. Appl. **8**, 259 (1973).
- [4] V. Leute and N. Volkmer, Z. Physikal. Chem. **144**, 145 (1985).
- [5] V. Leute, A. Behr, C. Hünting, and H. M. Schmidtke, Solid State Ionics **68**, 287 (1994).
- [6] V. Leute, Ber. Bunsenges. Phys. Chem. **93**, 548 (1989).
- [7] V. Leute and R. Schmidt, Z. Physikal. Chemie **172**, 81 (1991).
- [8] N. Kh. Abrikosov, V. F. Bankina, L. V. Poretskaya, L. E. Shelimova, and E. V. Skudnova, "Semiconducting II-VI, IV-VI, and V-VI Compounds", Plenum Press, New York 1969.
- [9] V. Leute and D. Menge, Z. Physikal. Chem. **176**, 65 (1992).
- [10] V. Leute and H.-J. Köller, Z. Physikal. Chem. **149**, 213 (1986).
- [11] M. R. Dombrugov and G. I. Zhovnir, Inorg. Mater. **24**, 121 (1988).
- [12] J. Steininger, J. Appl. Phys. **41**, 2713 (1970).
- [13] V. Leute and D. Menge, Z. Physikal. Chem. **176**, 47 (1992).
- [14] M. Shamsuddin, Mater. Res. Bull. **12**, 7 (1977).
- [15] G. H. Aylward and T. J. V. Finlay, Datensammlung Chemie, VCH, Weinheim 1975.
- [16] Ya. N. Nasirov and Ya. S. Feiziev, Neorganicheskie Materialy **5**, 380 (1969).
- [17] J. Emsley, The Elements, Clarendon Press, Oxford 1989.